The transcription factor MZF1 differentially regulates murine *Mtor* promoter variants linked to tumor susceptibility

Received for publication, June 13, 2019, and in revised form, September 18, 2019 Published, Papers in Press, September 23, 2019, DOI 10.1074/jbc.RA119.009779

Shuling Zhang[‡], Wei Shi[§], Edward S. Ramsay[‡], Valery Bliskovsky[‡†], Adrian Max Eiden[‡], Daniel Connors[‡], Matthew Steinsaltz[‡], Wendy DuBois[‡], and Beverly A. Mock[‡1]

From the [‡]Laboratory of Cancer Biology and Genetics, Center for Cancer Research, and the [§]Vaccine Research Center, NIAID, National Institutes of Health, Bethesda, Maryland 20892

Edited by Xiao-Fan Wang

Mechanistic target of rapamycin (MTOR) is a highly conserved serine/threonine kinase that critically regulates cell growth, proliferation, differentiation, and survival. Previously, we have implicated *Mtor* as a plasmacytoma-resistance locus, *Pctr2*, in mice. Here, we report that administration of the tumor-inducing agent pristane decreases *Mtor* gene expression to a greater extent in mesenteric lymph nodes of BALB/cAnPt mice than of DBA/2N mice. We identified six allelic variants in the *Mtor* promoter region in BALB/cAnPt and DBA/2N mice. To determine the effects of these variants on *Mtor* transcription, we constructed a series of luciferase reporters containing these promoter variants and transfected them into mouse plasmacytoma cells. We could attribute the differences in *Mtor* promoter activity between the two mouse strains to a C → T change at the −6 position relative to the transcriptional start site Tssr 40273; a T at this position in the BALB promoter creates a consensus binding site for the transcription factor MZF1 (myeloid zinc finger 1). Results from electrophoretic mobility shift assays and DNA pulldown assays with ChIP-PCR confirmed that MZF1 binds to the *cis*-element TGGGGA located in the −6/−1 *Mtor* promoter region. Of note, MZF1 significantly and differentially down-regulated *Mtor* promoter activity, with MZF1 overexpression reducing *Mtor* expression more strongly in BALB mice than in DBA mice. Moreover, MZF1 overexpression reduced *Mtor* expression in both fibroblasts and mouse plasmacytoma cells, and *Mzf1* knockdown increased *Mtor* expression in BALB3T3 and NIH3T3 fibroblast cells. Our results provide evidence that MZF1 down-regulates *Mtor* expression in pristane-induced plasmacytomas in mice.

The conserved serine/threonine kinase mechanistic target of rapamycin (MTOR),[2] a downstream effector of the phosphatidylinositol 3-kinase/AKT pathway, forms at least two distinct multiprotein complexes, mTORC1 and mTORC2, which function in regulating cell growth, proliferation, differentiation, and survival (1–3). The core complexes include mLST8 (mammalian lethal with Sec13 protein 8), TTT (TEL2 (telomere maintenance 2)–TTI1(yeast homolog to KIAA0406)-TTI2), and either RAPTOR (regulatory associated protein with MTOR) to form mTORC1 or RICTOR (rapamycin-insensitive companion of MTOR) to form mTORC2 (3). Several additional proteins bind each of the two complexes. In addition, a new MTOR complex has recently been identified in which MTOR associates with mEAK-7 (mammalian enhancer-of-*akt*-1–7) and mLST8 independent of RAPTOR or RICTOR binding and functions as an upstream regulator of S6K2 and 4E-BP1 activities (4).

Significant progress has been made in understanding how MTOR serves as a sensor that integrates a variety of exogenous cues to regulate cellular growth and metabolism, in both physiological and pathological conditions, including cancer. Deregulation of multiple elements in MTOR pathways has been reported in numerous cancers. Inhibition of MTOR kinase activity has been the aim of intense anti-cancer clinical research, because MTOR is often overexpressed or mutated in cancer cells (1).

Cancer development in human populations is a complex genetic trait. Pristane-induced plasmacytomas (PCTs) in mice provide an animal model system relevant to several human B cell malignancies, predominantly non-Hodgkin's lymphomas, including human plasma cell tumors, Burkitt's lymphoma, and multiple myeloma. In our previous studies, *Mtor* was identified as a tumor susceptibility/resistance gene in the pristane-induced PCT mouse model (5). BALB/cAnPt (BALB) mice are susceptible to PCT induction, whereas DBA/2N (DBA) and most other strains of mice are resistant (6). BALB mice carry a rare hypomorphic allele— encoding cysteine instead of a conserved arginine, R628C, in the HEAT domain of *Mtor*—leading to less kinase activity (5) and less phosphorylation of EIF4EBP1 (7) compared with the DBA allele. Furthermore, constitutive reductions in *Mtor* alter cell size, immune cell development, and antibody production (7), as well as limiting humoral responses *in vivo* (8, 9).

This work was supported by the Intramural Research Program of the National Institutes of Health, National Cancer Institute. The authors declare that they have no conflicts of interest with the contents of this article. The content is solely the responsibility of the authors and does not necessarily represent the official views of the National Institutes of Health.

This article contains Tables S1 and S2 and Figs. S1–S4.

The nucleotide sequence(s) reported in this paper has been submitted to the DDBJ/GenBank™/EBI Data Bank with accession number(s) MN076323.1 and MN076324.1.

[†] Deceased

[1] To whom correspondence should be addressed: 37 Convent Dr., Bldg. 37, Rm. 3146, Bethesda, MD 20892-4852. Tel.: 240-760-6942; E-mail: mockb@mail.nih.gov.

[2] The abbreviations used are: MTOR, mechanistic target of rapamycin; PCT, plasmacytoma; MLN, mesenteric lymph node; CRE, *cis*-regulatory element; qPCR, quantitative PCR; nt, nucleotide(s); NRLB, No Read Left Behind; SNP, single-nucleotide polymorphism; EMSA, electrophoretic mobility shift assay; NE, nuclear extract; Rluc, *Renilla* luciferase reporter.

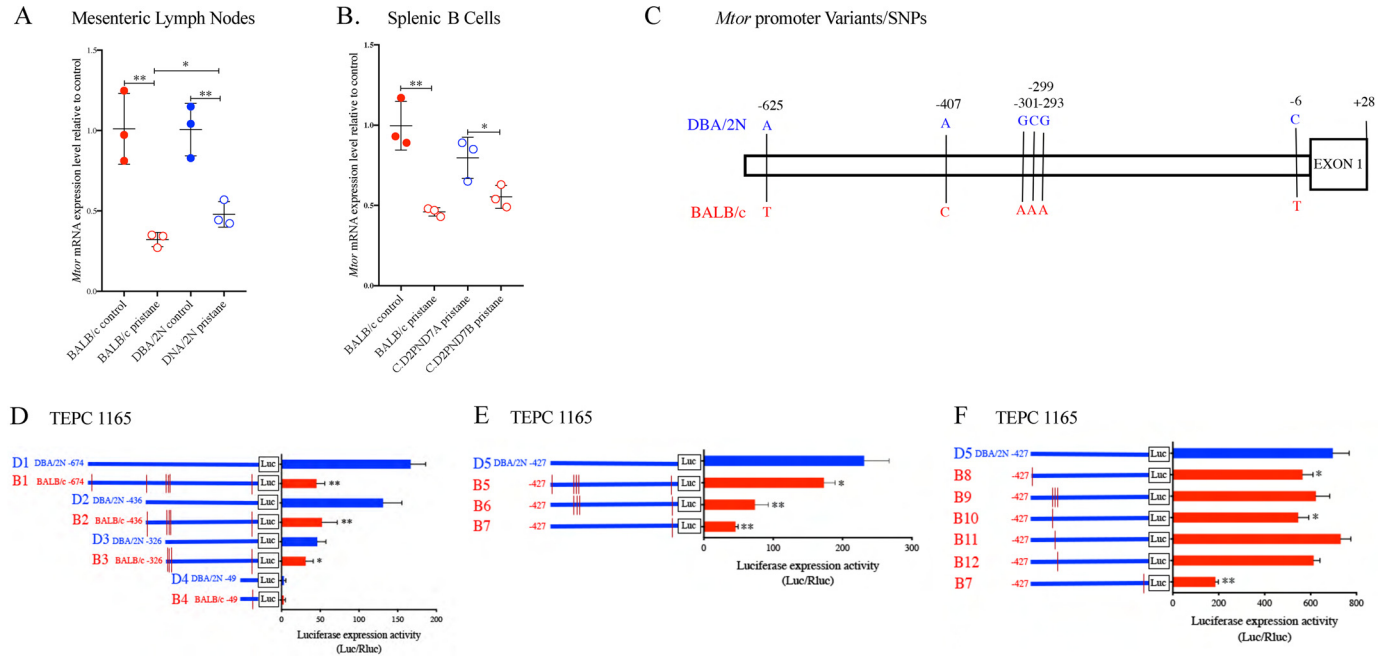

Figure 1. Mtor expression, promoter variants, and differential promoter activity in mouse strains. *A*, qPCR assay for *Mtor* mRNA expression in MLNs from BALB/cAnPt (BALB) and DBA/2N (DBA) mice. *Solid symbols* represent expression in PBS injected control mice, and *open symbols* represent expression in mice injected with pristane. The means ± S.D. of three independent assays ($n = 3$) represent fold change relative to the control (normalized by 18S). *, $p < 0.05$; **, $p < 0.01$. *B*, qPCR assay for *Mtor* mRNA expression in splenic B cells from a series of BALB congenic strains: C.D2Pnd(Nppa)7A carries a segment of DBA chromatin surrounding *Nppa*, including the *Mtor* locus from DBA and C.D2Pnd7B mice, which also carries a segment of DBA chromatin surrounding *Nppa* from DBA mice, but has *Mtor* sequences from BALB mice. *Solid symbols* represent expression in PBS injected control mice, and *open symbols* represent expression in mice injected with pristane; *red* indicates BALB, and *blue* indicates DBA. The means ± S.D. of three independent assays ($n = 3$) represent fold change relative to BALB/c control mice (normalized by 18S). *, $p < 0.05$; **, $p < 0.01$. *C*, schema showing the six different nucleotide variants in the *Mtor* promoter (from −674 to +28, relative to Tssr 40273) between BALB and DBA mice. Dual-Luciferase reporter assays to identify allelic variants in the *Mtor* promoter responsible for its down-regulation. *D*, Luciferase activity in serially truncated versions of the BALB and DBA *Mtor* promoter. The *t* tests indicated significance in the difference in luminescence between BALB and DBA. *E* and *F*, chimeric versions of the *Mtor* promoter (−427 to −1) differing at one or more of five nucleotide variants were tested for luciferase activity. The *t* tests indicated a significant difference in luminescence (all constructs were compared with D5 (DBA/2N)). *Numbers* indicate nucleotide positions with respect to +1 as the transcriptional start site. In all luciferase assays: 9 μg of the mTOR promoter-pGL3-luc reporter construct and 1 μg of pRL-SV40-Rluc plasmid DNA (transfection control) were used to co-transfect TEPC1165 (PCT) cells using electroporation (2 million cells per well in 6-well plates). The cells were harvested 24 h post-transfection for the Dual-Luciferase assay. Each data point is the mean ± S.D. (*error bar*) of three independent assays ($n = 3$). *, $p < 0.05$; **, $p < 0.01$. *Red lines* indicate the presence of the BALB variant at that nucleotide.

In the current study, decreased levels of *Mtor* mRNA and protein expression were found in the mesenteric lymph nodes (MLNs) of mice after intraperitoneal injection of pristane. *Mtor* expression was more reduced in BALB than in DBA mice or BALB congenic mice carrying a DBA/2 allele of mTOR. Sequencing of the *Mtor* promoter region revealed six allelic variants between BALB and DBA mice in the region from −674 to +28 relative to Tssr 40273. We therefore sought to identify the relevant *cis*-regulatory element (CRE) and the transcription factor that could repress *Mtor* and contribute to its differential expression in MLNs from BALB and DBA mice after pristane induction.

Results

Transcription of the Mtor gene is differentially down-regulated by pristane treatment in plasmacytoma-susceptible versus plasmacytoma-resistant mice

Pristane treatment led to a significant reduction of *Mtor* mRNA levels in the MLNs of mice 18 days postinjection with pristane *versus* PBS (RT-qPCR; Fig. 1*A*). *Mtor* expression was reduced ~3-fold in BALB, which was significantly greater than the ~2-fold reduction in DBA. Similarly, in a separate experiment, pristane treatment of a pair of BALB congenic strains led to lower *Mtor* levels in splenic B cells isolated from tumor-susceptible C.D2Pnd7B mice harboring the BALB allele of *Mtor*, compared with levels in B cells from tumor-resistant, C.D2-Pnd7A mice harboring the DBA allele (Fig. 1*B*). Both of these strains of mice carry BALB/c alleles of genes throughout the genome (99% BALB), and 1% of their genome are from DBA Chr 4 near the *Mtor* locus. The segments introgressively backcrossed onto BALB contain the DBA allele of *Mtor* in the C.D2-Pnd7A mouse and a small region of chromosome 4 adjacent to, but not including DBA *Mtor*, in the C.D2-Pnd7B mouse (5).

Determination of allelic variants in the Mtor promoter between BALB and DBA mice and identification of MZF1 CREs in the Mtor promoter

To analyze the differential expression of *Mtor*, BALB and DBA *Mtor* promoters were cloned and sequenced (GenBank™ accession numbers: MN076323.1 and MN076324.1). Six allelic variants were identified in the promoter between positions −674 and +28 (the transcriptional start site Tssr 40273 is designated +1; see sequence alignment schema in Fig. 1*C* and Figs. S1*A* and S2). The allelic variants between DBA and BALB are at the following positions: −625 (A/T), −407 (A/C), −301 (G/A), −299 (C/A), −293 (G/A), and −6 (C/T).

Versions of BALB and DBA mTOR promoters from position −674 to +28 were cloned into the pGL3 vector (Table S2 and

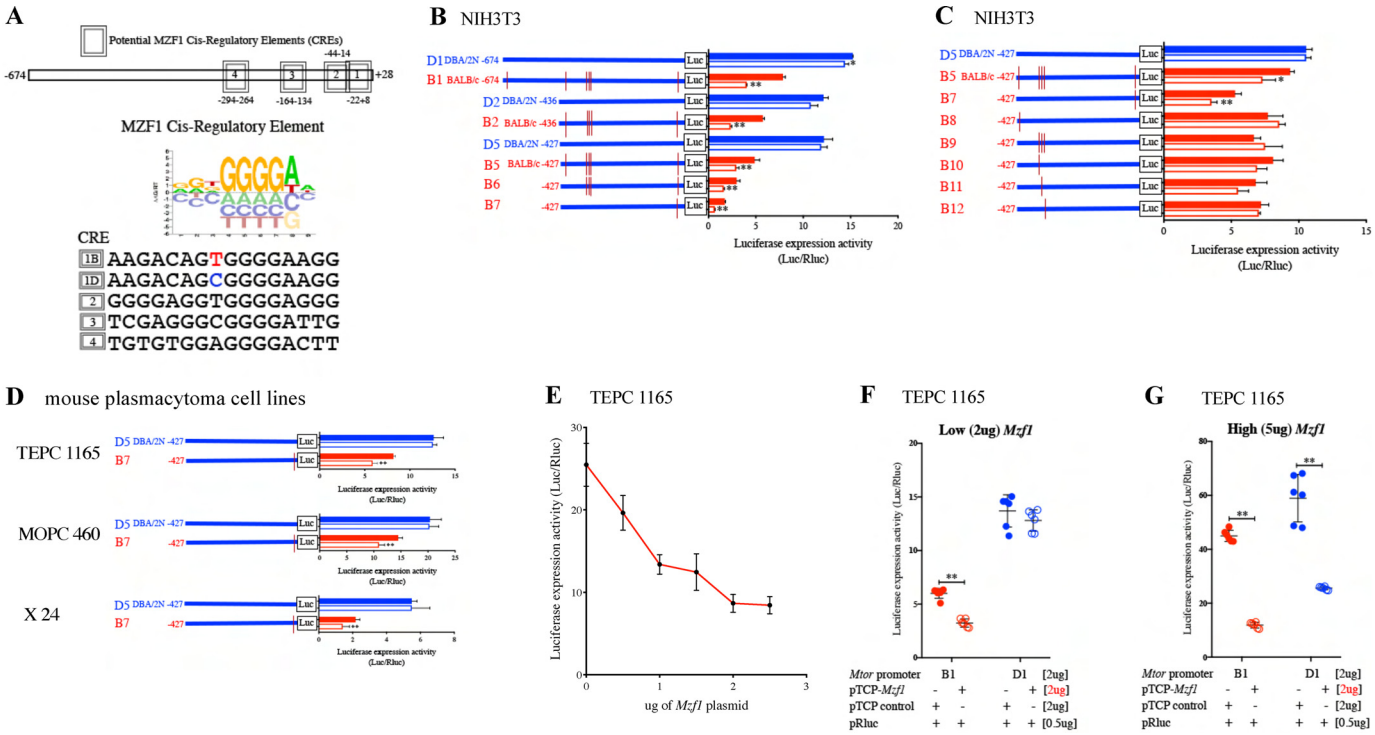

Figure 2. MZF1 *cis*-regulatory elements and differential promoter activity associated with the −6 nucleotide variant in the *Mtor* promoter. *A*, schema of four potential MZF1 CREs in the *Mtor* promoter (−674 to +28). The conserved nucleotides were identified using the recognition model/algorithm denoted as NRLB. *B* and *C*, Luciferase activity assays in NIH3T3 cells transfected with serially truncated (*B*) or chimeric (*C*) versions of the *Mtor* promoter in pGL3-luc (24-well plates) along with a pTCP plasmid containing full-length cDNA of *Mzf1* (1:1 ratio, 2 μg/well each), and pRL-SV40-Rluc (0.5 μg/well) to provide an internal control for normalization of luciferase activity. *D*, Luciferase activity of the D5 and B7 *Mtor* promoters co-transfected in mouse plasmacytoma cell lines (TEPC1165, MOPC460, and XRPC24) with *Mzf1* (2 μg). *E*, dose responsiveness of luciferase activity (Luc/Rluc) of the *Mtor* promoter (pGL3-B1 plasmid, 2 μg/well) after co-transfection by electroporation with pRL-SV40-Rluc plasmid (0.5 μg/well) and a *Mzf1* expression plasmid (pTCP-*Mzf1*, concentration ranging from 0 to 2.5 μg/well) into TEPC1165 plasmacytoma cells (2×10^6 cells/well in 6-well plates). *F* and *G*, Luciferase activity of the B1 and D1 *Mtor* promoters (pGL3-B1 plasmid (2 μg/well)/*Renilla* luciferase values obtained from co-transfection by electroporation with pRL-SV40 plasmid DNA (0.5 μg/well) and either pTCP-*Mzf1* in low concentrations (*F*, 2 μg/well) or in high concentrations (*G*, 5 μg/well) in TEPC1165 plasmacytoma cells (2×10^6 cells/well in 6-well plates). Cells were harvested at 24 h post-transfection in the Dual-Luciferase assays. Each data point is the mean ± S.D. of at least three independent assays ($n = 6$ or 3). The *t* tests indicate significant differences in luminescence between control (pTCP empty vector, *solid bars* or *circles*) *versus* *Mzf1* overexpression (pTCP-*Mzf1*, *open bars* or *circles*). **, $p < 0.01$; *, $p < 0.05$. *Red*, BALB; *blue*, DBA.

Fig. S1), and luciferase assays were used to measure promoter activity. These constructs were used to create a series of truncated and chimeric plasmids to evaluate the six divergent nucleic acids in the BALB *versus* DBA *Mtor* promoter. The results indicated that the DBA *Mtor* promoter was 3-fold more active than the BALB promoter when transfected into mouse plasmacytoma cell lines, TEPC1165 (10) (Fig. 1*D*), MOPC460 (Fig. S1*E*), and XRPC24 (X24; Fig. S1*F*), and the difference in promoter activity was attributable to the C-to-T divergence at the −6 nucleotide (nt) position (Fig. 1, *E* and *F*).

The GTGGGGAA sequence surrounding the −6 nt site in the BALB/c *Mtor* promoter is an established consensus MZF1-binding site (MZF1 CRE; CRE1B (nt −22 to +8, named 1B for the BALB *Mtor* promoter)) with 100% sequence identity based on MatInspector analysis and the recognition model of No Read Left Behind (NRLB) (11–14) (Fig. 2*A*). The sequence (GCGGGGAA) at the same site in the DBA/2N *Mtor* promoter has 90% identity with the MZF1 binding site (MZF1 CRE1D for the DBA allele in the promoter). Co-transfection of *Mzf1* along with the *Mtor* promoter variants (deletions and chimeras) in NIH3T3 cells led to greater down-regulation of promoter activity in constructs carrying the BALB allele (T) *versus* the DBA allele (C) at the −6 nt position, as measured by luciferase activity (Fig. 2, *B* and *C*). There were three other potential MZF1 CREs found (nt −14 to −44, −164 to −134, and −294 to −264) with at least 85% sequence identity (Fig. 2*A* and Fig. S2), but they did not affect *Mtor* promoter activity (Fig. 2, *B* and *C*). Luciferase activity of the B7 promoter (T at −6) was repressed by co-transfection with Mzf1; in contrast, D5 promoter (C at −6) activity was not affected (Fig. 2, *C* and *D*). This was seen in both fibroblasts and plasmacytoma cells.

MZF1 reduced the luciferase activity of the *Mtor* promoter in a dose-dependent manner (Fig. 2, *E*–*G*). As the amount of *Mzf1* plasmid was increased in co-transfections with the BALB *Mtor* promoter (B1 depicted in Figs. 1*D* and 2*B*) in TEPC1165 plasmacytoma cells, promoter activity was decreased (Fig. 2*E*). Furthermore, low doses of the *Mzf1* plasmid did not significantly down-regulate the DBA D1 promoter (which has a single-nucleotide polymorphism (SNP) relative to BALB) (Fig. 2*F*); only the high dose of *Mzf1* was able to down-regulate the DBA (D1 depicted in Figs. 1*D* and 2*B*) *Mtor* promoter (Fig. 2*G*).

MZF1 binds to the Mtor promoter CRE encompassing the variant nucleotide (−6) closest to the transcription start site, designated Tssr 40273

A series of electrophoretic mobility shift assays (EMSAs) were carried out with nuclear extracts (NEs) from either

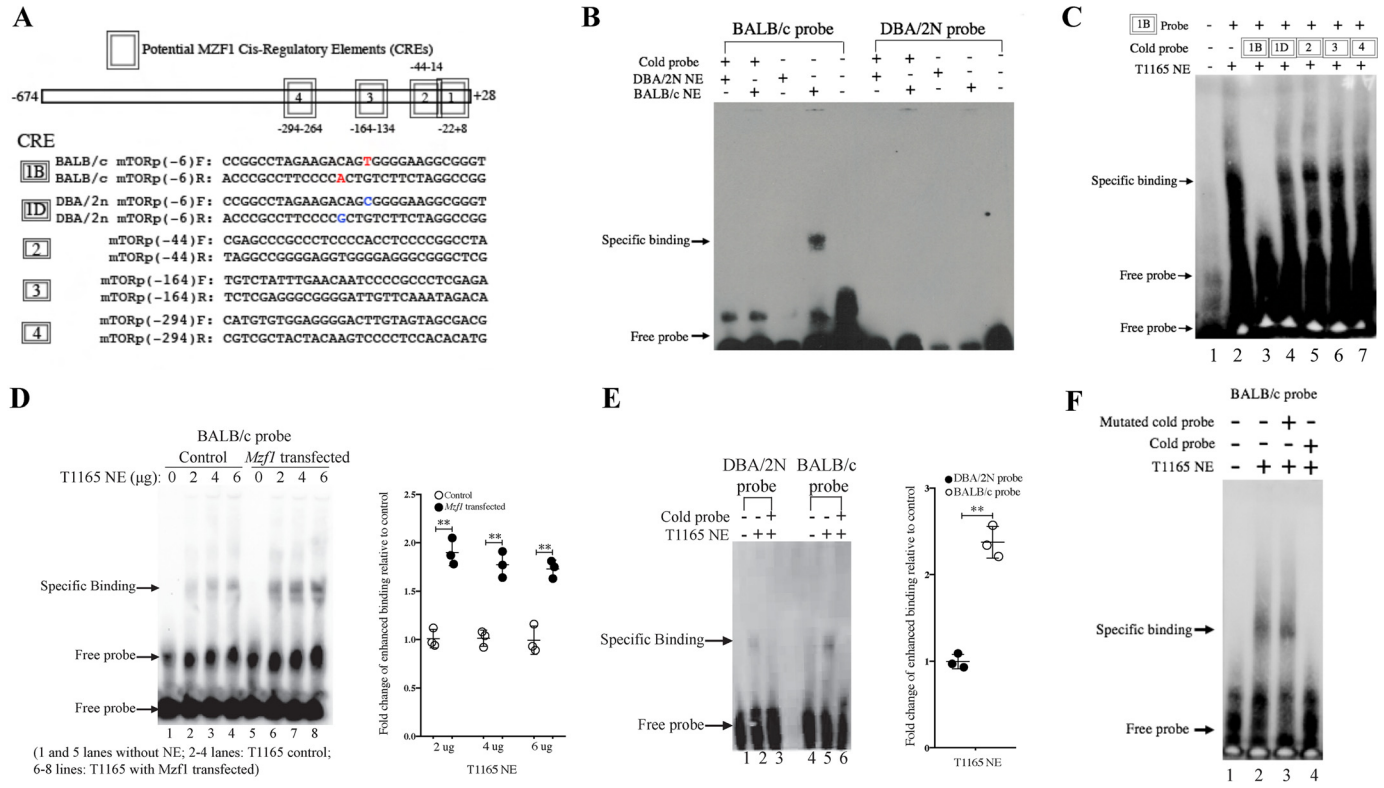

Figure 3. MZF1 binds to the predicted CRE at the −6 nucleotide position in the BALB *Mtor* promoter. *A*, schema of BALB and DBA probes (sequences) for EMSAs. *B*, representative EMSA of BALB and DBA NEs isolated from splenic B cells and incubated (20 min at room temperature) with BALB (T at −6) and DBA (C at −6) *Mtor* promoter probes (*arrow* indicates specific binding of the BALB probe to BALB NE). This experiment was repeated at least three times. *C*, representative EMSA of TEPC1165 NE incubated with unlabeled probes shown in *A* in addition to the labeled BALB *Mtor* probe (*1B*); only the unlabeled 1B probe was able to effectively compete with the labeled probe for binding (*lane 3*). This experiment was repeated three times. *D*, representative EMSA of TEPC1165 NE incubated with the BALB *Mtor* probe shows enhanced binding of the BALB probe to *Mzf1* transfected *versus* control (empty vector) cells. Specific binding of MZF1 was quantified (means ± S.D.) from three independent assays for control *versus Mzf1*-transfected (fold change relative to control and normalized by free probe intensity. **, $p < 0.01$. *E*, representative EMSA of TEPC1165 NE with preferential binding to BALB *versus* DBA *Mtor* probes. *Lanes 2* and *5* were quantified and means + S.D. of three independent assays are shown (fold change relative to control and normalized by free probe intensity. **, $p < 0.01$. *F*, representative EMSA of TEPC1165 NE incubated with mutant cold (unlabeled, 5′-CCGGCCTAGAAGACAGTTTTTAAGGCGGGT-3′) probe did not compete away binding of the BALB *Mtor* probe. A 200-fold excess of cold probe was used in competition assays. The data were consistent among three separate experiments.

BALB and DBA splenic B cells (Fig. 3*B*) or TEPC1165 plasmacytoma cells (Fig. 3, *C–F*) to examine the binding of MZF1 to its putative CREs (Fig. 3*A*) in the *Mtor* promoter. NEs isolated from splenic B cells, TEPC1165 cells, or TEPC1165 cells with *Mzf1* transfection were used as the source of MZF1 protein. Formation of a DNA–protein complex could only be detected with CRE1B (T allele at −6 nt in BALB) incubated with NE from BALB splenic B cells (Fig. 3*B*). The addition of a 200-fold molar excess of unlabeled CRE1B "cold" probe abolished formation of the complex (Fig. 3*C*, *lane 3*). In contrast, excess unlabeled CRE1D (contains C allele at −6 SNP in DBA) or CRE2-4 did not completely abolish complex formation (Fig. 3*C*, *lanes 4–7*). Biotin-labeled probes for CRE2-4 did not detect any specific protein complex (data not shown) when performing EMSA with NE of T1165 or splenic B cells. Complex formation was enhanced in a dose-dependent manner in NE of *Mzf1* transfected TEPC1165 cells (Fig. 3*D*). The BALB probe (CRE1B) bound more efficiently than the DBA probe in NE from TEPC1165 (Fig. 3*E*), and unlabeled mutated probe (unlabeled 5′-CCGGCCTAGAAGACAGTTTTTAAGGCGGGT-3′) could not compete with the BALB/c probe (CRE1B) for the formation of a protein complex with T1165 NE (Fig. 3*F*, *lane 3*).

MZF1 interacts with an Mtor promoter CRE and down-regulates Mtor expression in vivo

To test whether MZF1 was recruited to the CRE including the −6 nt site of the *Mtor* promoter, ChIP analysis was performed with PCT (TEPC1165) cells. ChIP-enriched DNA carrying CRE1B (MZF1 CRE in BALB promoter) was amplified by PCR (Fig. S3, *A* and *B*) and quantified by qPCR (Fig. 4*A* and Fig. S3, *C* and *D*). There are three Tssr sites (40273, 40274, and 40275) by CAGE analysis/FANTOM annotation. The ChIP-PCR analyses covers all three Tssr sites.

Anti-MZF1 antibody, but not IgG antibody (negative control), precipitated the MZF1 CRE1B from TEPC1165 cells. MZF1 bound the MZF1 CRE1B in the nt −22 to +8 region of the *Mtor* promoter *ex vivo*.

Mzf1 mRNA (Fig. 4*B*) and MZF1 protein (Fig. S4) levels were increased in MLNs from pristane primed BALB and DBA mice. In contrast, *Mtor* mRNA (Fig. 4*B*) and MTOR protein (Fig. S4) levels were decreased (lower *Mtor* levels) in B cells from BALB (Fig. 4*B*). Furthermore, when *Mzf1* was overexpressed in TEPC1165, BALB3T3 (T allele at *Mtor* −6 nt), or NIH3T3 (C allele at *Mtor* −6 nt) cells, there were concomitant decreases in *Mtor* mRNA and protein levels (Fig. 4, *C* and *D*). *Mtor* levels

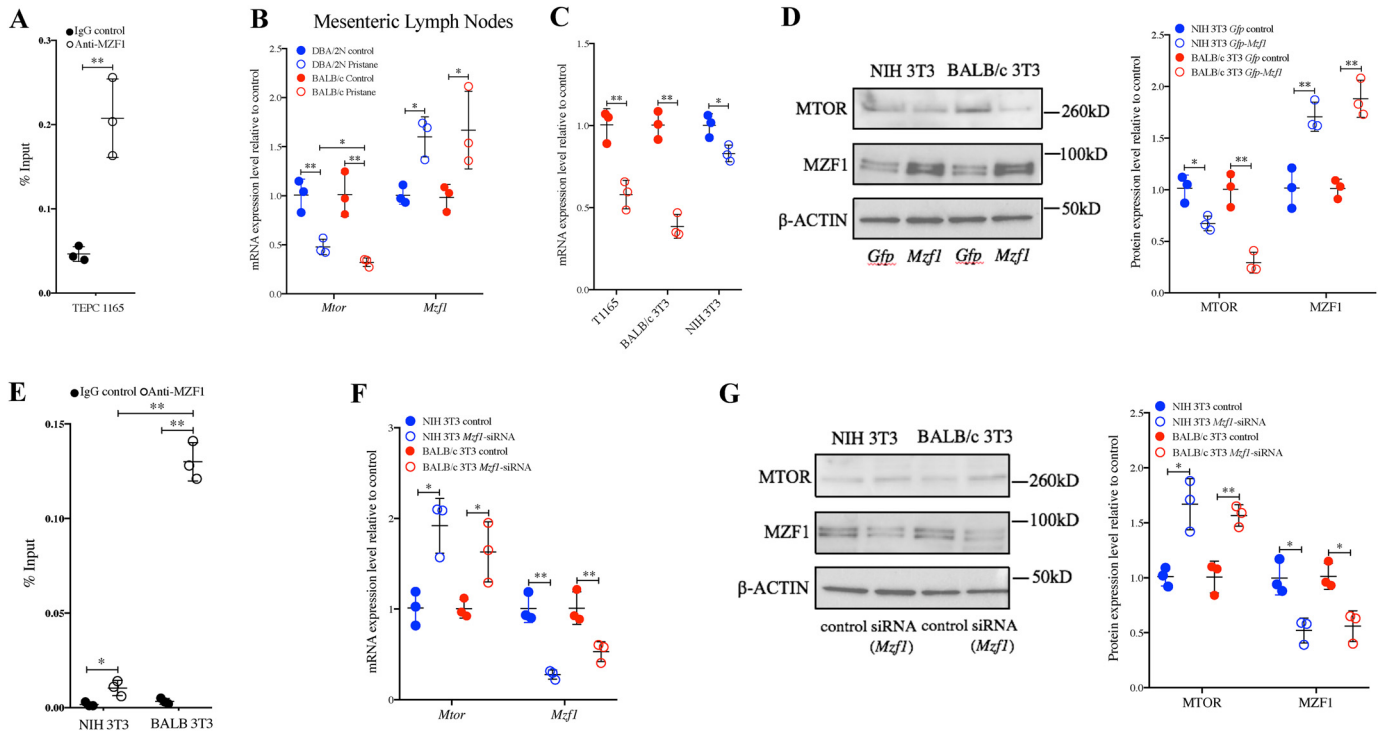

Figure 4. MZF1 interacts with *Mtor* promoter CRE and regulates the expression of *Mtor* in cells. *A*, ChIP-qPCR analysis of the binding between MZF1 and its CRE at the −6 nucleotide position on the *Mtor* promoter in TEPC1165 cells. The percentage of input represents the enrichment of DNA pulled down using IgG control or anti-MZF1 antibody in three independent experiments ($n = 3$, mean ± S.D.). *, $p < 0.05$; **, $p < 0.01$. *B*, qPCR analysis of *Mtor* and *Mzf1* mRNA expression in MLNs from BALB and DBA mice after pristane treatment. Fold changes are shown relative to the control samples and normalized by 18S RNA. *C* and *D*, *Mtor* mRNA (*C*) and MTOR (*D*) protein levels decrease preferentially in BALB3T3 *versus* NIH3T3 cells with overexpression of *Mzf1* (transfected with pMYs-MZF1-IRES-GFP or empty pMYs-IRES-GFP vector). *E*, ChIP-qPCR analysis after overexpression of *Mzf1* in NIH3T3 (C at −6) and BALB3T3 (T at −6) cells. The percentage of input represents the enrichment of DNA pulled down using IgG control or anti-MZF1 antibody in three independent experiments ($n = 3$, mean ± S.D.) *, $p < 0.05$; **, $p < 0.01$. *F* and *G*, *Mtor* mRNA (*F*) and MTOR (*G*) protein levels (representative Western blotting) increase in BALB3T3 and NIH3T3 cells after knockdown of *Mzf1* expression (transfected with *Mzf1* siRNA or siRNA negative control). RNA and protein lysates were isolated from transfected cells 48 h post-transfection. The results of qPCR analysis of *Mtor* and *Mzf1* mRNA expression represent the means ± S.D. of three independent assays ($n = 3$) (fold change relative to the control and normalized by 18S). *, $p < 0.05$; **, $p < 0.01$. MTOR and MZF1 protein expression (Western blotting) are estimated as fold change compared with their controls (normalization with β-Actin).

were reduced to an even greater extent in cells containing the BALB T allele, compared with the C allele at nt −6. ChIP-qPCR analyses of DNA from NIH3T3 and BALB3T3 cells revealed a 13-fold increase in the recruitment of MZF1-CRE1B in BALB3T3 cells compared with MZF1-CRE1D in NIH3T3 cells (Fig. 4*E*).

Consistent with MZF1 regulation of the *Mtor* promoter, siRNA-mediated knockdown of *Mzf1* resulted in increased *Mtor* mRNA (Fig. 4*F*) and MTOR protein (Fig. 4*G*) levels. These findings are consistent with MZF1 functioning as a repressor of *Mtor* transcription by binding to its CRE surrounding the −6 nt polymorphic site.

Discussion

Promoter activity studies involving a series of *Mtor* promoter region deletion and chimeric plasmids, coupled with DNA-binding assays, identified MZF1 as a transcription factor capable of repressing *Mtor* transcription. The MZF1 CRE at nt −22 to +8 encompassed a variant SNP (T in BALB and C in DBA) at nt −6. The BALB variant (T) at the −6 position from the Tssr 40273 start site was a direct match with the MZF1 consensus binding site, and MZF1 demonstrated preferential binding to the BALB allele. ChIP assays confirmed MZF1 recruitment to the *Mtor* promoter. Our studies provide insight into understanding the genetic differences between BALB and DBA *Mtor* promoters. Further analyses would be required to gain a complete understanding of *Mtor* regulation.

Pristane treatment, used to induce PCTs, caused *Mzf1* levels to increase and *Mtor* levels to decrease. Importantly, pristane-induced *Mzf1* levels were similar in BALB and DBA mice, whereas the pristane-induced decrease in *Mtor* was greater in BALB and the PCT-susceptible congenic strain, Pnd7B, than in DBA. Our *in vitro* studies to overexpress or silence *Mzf1* demonstrated concomitant changes in *Mtor* expression. When *Mzf1* was overexpressed, BALB *Mtor* promoter activity was repressed, whereas siRNA experiments that decreased *Mzf1* levels resulted in increased *Mtor* expression. Thus, our studies have identified MZF1 as a new transcriptional repressor of *Mtor* in cells exposed to the inflammatory agent pristane.

MZF1 is a member of the SCAN–zinc finger family of transcription factors (11) and can function both as trans-activator and trans-repressor depending on the intracellular environment (15–21). Although the role of MZF1 was initially studied in myeloid differentiation and leukemia, the factor now appears to be involved in the pathogenesis of several solid tumors (22). The contribution of MZF1 to tumorigenesis is diverse, because it may induce oncogenic or tumor suppressor effects in hema-

topoietic and nonhematopoietic cells. MZF1 has been implicated in mediating the migration and invasion of cancer cells by suppressing the activity of certain gene promoter regions *in vivo* and *in vitro* (17). The relative oncogenic activity of MZF1 is determined by the aggregated effects produced by the increases and decreases in gene expression, phosphorylation and SUMOylation modifications, and co-activating and co-repressing molecules (22).

The MTOR signaling pathway controls key cellular processes, such as metabolism, growth, motility, and survival, and is a frequently dysregulated pathway in cancer (3). Aberrant activation of the pathway via multiple mechanisms has been detected in a range of tumor types, including diverse genomic alterations of the pathway's components (23). Somatic cancer-associated mutations in *MTOR* are often hyperactivating (24), and at least one promoter polymorphism (rs2295080 at nt −64) has been associated with an altered risk of developing renal (25), gastric (26), and genitourinary cancers, as well as acute childhood leukemia (27). Previously, only one transcription factor, NFE2L2 (nuclear factor erythroid 2-related factor, also called NRF2), has been reported to regulate *Mtor* and only when the phosphatidylinositol 3-kinase pathway is intact (28). The promoter sequence surrounding the rs2295080 polymorphism does not have putative consensus binding sites for either NFE2L2 or MZF1.

Our studies suggest that the amount of MZF1 protein is an important driver in the differential regulation of *Mtor* promoter variants, as evidenced by the ability of low-dose overexpression of *Mzf1* to preferentially lower *Mtor* promoter levels associated with the BALB T allele. The *Mtor* promoter carrying the DBA C allele was only repressed by high-dose overexpression of *Mzf1*, likely because the DBA promoter does not have the optimal consensus binding site present in the BALB promoter. These data, coupled with our previous studies on *Mtor* in PCT development, reveal that BALB mice have both a coding region polymorphism (nt C1977T; AA R628C) (5), which lowers its kinase activity, and now at least one identified functional SNP that can, in addition, contribute to lower *Mtor* gene expression in BALB mice.

This compound allelic variation in both *Mtor* coding and regulatory sequences, along with previously reported allelic variants in *Cdkn2a* (exon 2: p16) coding (29) and promoter (30) sequences, contributes to the complex genetics associated with PCT susceptibility in BALB mice (6). Thus, hypomorphic activity of BALB *Cdkn2a* (p16) and *Mtor* alleles is associated with tumorigenesis, suggesting that both p16 and *Mtor* can act as tumor suppressors in PCT development in an allele-dependent manner. Although this may be expected for p16, which is widely recognized as a tumor suppressor, it is counter to the prevailing notion that *Mtor* activity is always growth-promoting. Interestingly, the G allele at rs2295080 in the human MTOR promoter is associated simultaneously with reduced promoter activity and increased risk for childhood acute leukemia but decreased risk for genitourinary cancers (27), thus highlighting the possibility of differential, tissue-specific susceptibility. Recently, Villar *et al.* (31, 32) have shown that the activation of mTORC1 by glutaminolysis during nutritional imbalance inhibits autophagy and induces apoptosis in cancer cells, thus supporting a tumor suppressor role under stress conditions. Furthermore, Villar *et al.* (31, 32) showed that the MTOR inhibitor, rapamycin, can actually block glutaminolysis-mediated apoptosis, leading to improved cancer cell survival. Thus, as in the murine pristane-induced PCT system, there appear to be human tumors where MTOR may play an inhibitory role.

Experimental procedures

Mice

Mice were maintained under conventional, closed barrier conditions at the National Cancer Institute under animal protocol LG-009. Experiments were conducted according to the institutional ethical guidelines for animal experiments and safety guidelines for gene manipulation experiments. Mesenteric lymph nodes were collected from 8-week-old BALB/cAn and DBA/2N mice, 18 days postinjection with pristane (0.5 ml). Pristane induces chronic inflammation in BALB/c mice (33). BALB/c congenic mice, C.D2-Pnd7A mice, and C.D2-Pnd7B mice were generated by introgressive backcrossing (N12) of segments of DBA DNA from Chr 4 onto the BALB background (34). C.D2-Pnd7A mice are relatively resistant to plasmacytoma induction and carry a segment of DBA DNA encompassing the *Mtor* locus; in contrast, C.D2-Pnd7B mice are as susceptible as BALB/c mice and carry a segment of DBA DNA adjacent to, but not including the *Mtor* locus (34). Splenic B cells were prepared from spleens of DBA and BALB/c congenic mice using the protocol for a CD45R(B220) MicroBeads kit (catalog no. 130-049-501, Miltenyi Biotec).

Reagents and antibodies

All the reagents were of analytical grade and purchased from Merck or Sigma–Aldrich. All primers and oligonucleotides were ordered from Eurofins Genomics. Restriction enzymes were purchased from New England Biolabs. The anti-MZF1 antibodies (sc-66991 for Western blotting and sc-66991x for ChIP assay plus control rabbit IgG; sc-2027) were purchased from Santa Cruz Biotechnology. Another anti-MZF1 antibody (Western blotting) was purchased from Abcam (ab64866). The anti-mTOR antibody (catalog no. 2972) and anti-β-actin antibody (catalog no. 4970) were from Cell Signaling Technology.

Cell culture

TEPC1165, MOPC460, and XRPC24, all mouse plasmacytoma cell lines induced in BALB/cAnPt mice (10) were grown in RPMI 1640 medium (Invitrogen) supplemented with 10% heat-inactivated fetal calf serum, 2 mM L-glutamine, 100 units/ml penicillin, 100 μg/ml streptomycin, 50 nM β-mercaptoethanol, and 5 ng/ml IL-6 (Sigma); XRPC24 cells were grown without IL-6. NIH3T3 and BALB3T3 cells were grown in the Dulbecco's modified Eagle's medium (Invitrogen) supplemented with 10% sterile-filtered fetal calf serum (Sigma), 100 units/ml penicillin, and 100 μg/ml streptomycin. All cells were cultured in at 37 °C in a humidified atmosphere containing 5% CO_2.

RNA extraction and qPCR

Total RNA was prepared using TRIzol reagent (Invitrogen) and purified using RNeasy PowerClean Pro cleanup kit (Qia-

gen). cDNAs were made with TaqMan RT reagents kit (Applied Biosystems: N808-0234). Expression of 18S rRNA from the same sample under analysis was used as an endogenous control. qPCR was performed using SYBR Green Master PCR Mix (part no. 4309155, ABI 7500, Applied Biosystems). The results are expressed as the ratios of values for treated samples to untreated samples and normalized to their 18S levels. Threshold values were converted to relative fold change using the $2^{-\Delta\Delta CT}$ method. The primer sets used for estimation of transcript levels for different genes are described in Table S1.

Cloning and sequencing of Mtor promoter

BALB/c and DBA/2N *Mtor* promoters were cloned following PCR amplification of tissue DNA from BALB/cAn and DBA/2N mice, respectively. The following primers were used to generate *Mtor* promoter fragments: forward, GCTCCGGCTATTGCCCGTTG, and reverse, GAGCAGATCCGCCAGCCTG. Fragments (921 bp) were then cloned into pCR-XL-TOPO vector (Invitrogen) to form pCR-TOPO-*Mtor*-1p-BALB/c and pCR-TOPO-*Mtor*-1p-DBA/2N. All sequencing was performed with BigDye terminator reagents (Applied Biosystems). The sequences were compared with (NC_000070.6 reference GRCm38.p4 C57BL/6J) reference database. GenBank™ accession numbers for BALB/cAnPt and DBA/2N Mtor promoters are MN076323.1 and MN076324.1, respectively. Promoter variant positions were counted from the transcription start site designated Tssr40273 based on FANTOM (functional annotation of the mammalian genome); there were two additional Tssrs (40274 and 40275) annotated for mouse *Mtor*.

Plasmid constructs

To functionally characterize the 5′-flanking region of the BALB/cAn and DBA/2N *Mtor* gene, a series of 5′ deletions or chimeric sequences in the −674 to +28 mostly upstream sequence were amplified using PCR from the subcloned pCR-TOPO-*Mtor*-1p-BALB/c and pCR-TOPO-*Mtor*-1p-DBA/2N plasmids containing *Mtor* promoter region sequences. The upstream primers contained a 5′-flanking MluI restriction enzyme site, whereas the downstream primers were flanked by a BglII site. The fragments of the 5′ region or chimeric sequences of the mTOR were inserted into the luciferase reporter plasmid, pGL3-basic vector (Promega). All plasmids were analyzed and confirmed by restriction digestion and DNA sequencing. The strategy and primer sets used for producing mTOR promoter reporter plasmids are described in Fig. S2 and Table S2.

Mouse *Mzf1* expression plasmids: pTCP expression vector and pTCP-Mzf1 (mouse Mzf1: BC129904) were purchased from TransOmic; pMYs-IRES-GFP retroviral vector was purchased from Cell Biolabs, and mouse *Mzf1* was subcloned into pMYs-IRES-GFP using EcoR1 and XhoI sites (forward, 5′-GGAAGAATTCATGGAGCTCCTGGAATCTGG-3′; and reverse, 5′-GGAACTCGAGCTACTCAGTGCTGTGGACAC-3′) and named pMYs-MZF1-IRES-GFP.

Luciferase assays

Mouse plasmacytoma cell lines were transiently transfected by electroporation (Amaxa nucleofector kit from Lonza Bioscience). NIH3T3 and BALB3T3 cells, grown in 24-well plates, were transfected using Lipofectamine 2000 or 3000 (Invitrogen). The cells were transfected with different reporter constructs carrying the *Mtor* promoter variants (driven by firefly luciferase, Luc) and harvested 24 h post-transfection for luciferase assays following Dual-Luciferase reporter assay system (Sigma) protocols; activity was measured with a FLUOstar Omega microplate reader (BMG Labtech). The pRL-SV40 (*Renilla* luciferase reporter, Rluc) was used as an internal transfection control and co-transfected with the reporter plasmids. Promoter activities are the means ± S.E. of 3–8 transfections (luciferase expression activity relative to *Renilla* luciferase activity, Luc/Rluc).

Western blots

Protein lysates were made with radioimmune precipitation assay lysis buffer (150 mM NaCl, 1.0% Nonidet P-40, 0.5% sodium deoxycholate, 0.1% SDS, 50 mM Tris, pH 8.0). Protein concentrations were determined by BCA reagent (Pierce). Proteins were mixed with 4× loading buffer (LDS sample buffer, Novex) containing 5% β-mercaptoethanol, and separated on 4–20% Tris-glycine polyacrylamide SDS-PAGE gels (Invitrogen); proteins were transferred to polyvinylidene difluoride membranes using the iBlot 2 dry blotting system (Invitrogen). The membranes were blocked with 5% (w/v) dry milk in TBST at room temperature for 1 h and then incubated with antibody with gentle rocking at 4 °C for overnight. After washing three times with TBST for 5 min each, the membranes were incubated with horseradish peroxidase–conjugated goat anti-rabbit IgG secondary antibody with gentle rocking at room temperature for 1 h. Membranes were washed five times with TBST for 5 min each and then detected with SuperSignal West Dura extended duration substrate (Thermo Fisher). In all experiments, β-actin was used as an internal reference, and ImageJ software was used for quantifying fluorescence of area integrated intensity.

Electrophoretic mobility shift assay

NEs were prepared from TEPC1165 cells and splenic B cells with NE buffer (NE-PER nuclear and cytoplasmic extraction kit; Pierce) supplemented with protease and phosphatase inhibitors. EMSA was performed using manufacturer's protocols (LightShift Chemiluminescent EMSA kit; Pierce). NEs were incubated for 20 min at room temperature in a final 20-μl reaction volume containing 10 mM Tris-HCl (pH 7.5), 50 mM KCl, 1 mM DTT, 0.2 mM EDTA, 2.5% (v/v) glycerol, 50 ng of poly(dI-dC), 0.05% Nonidet P-40, and 20 fmol of Biotin 3′-labeled oligonucleotide probe in the absence or presence of various competitors (200-fold cold probes). The reaction products were electrophoresed on a 6% nondenaturing polyacrylamide gel in TBS buffer. The gels were transferred to nylon membranes and cross-linked at 120 mJ/cm^2 using a UV cross-linker equipped with 254-nm bulbs and visualized using detection of Biotin-labeled DNA according to the manufacturer's protocols (LightShift Chemiluminescent EMSA kit (Pierce)). For quantitation, the free probe band was used as an internal reference, and ImageJ software was used to quantify the fluorescence of area-integrated intensity.

ChIP assay

ChIP experiments were performed according to manufacturer's instructions (Pierce agarose ChIP kit) using anti-MZF1 antibody and normal rabbit IgG as a negative control with TEPC1165, NIH3T3, and BALB3T3 cells. In brief, the ChIP experiment was performed to detect the effects of MZF1 on the promoter activity of *Mtor* in the cell lines. The cells were cross-linked with 1% formaldehyde for 10 min at room temperature. Glycine was added to terminate the fixation, and cells were washed and collected with ice-cold PBS. The cells were collected, and the cell pellets were broken up with membrane extraction buffer containing protease/phosphatase inhibitors. The nuclei were collected and digested with MNase. Digested chromatin was collected by centrifugation. An immunoprecipitation experiment was conducted following the manufacturer's instructions for the Pierce agarose ChIP kit (Thermo Scientific). Five μg of either rabbit anti-MZF1 antibody or normal rabbit IgG were used in immunoprecipitation reactions for 2 h at 4 °C with mixing. The antibody–protein–DNA complex was enriched by incubation with ChIP grade protein A/G–agarose beads for 1.5 h at 4 °C with mixing. The bound DNA was purified following the kit's instructions. Immunoprecipitated genomic DNA fragments were amplified and quantified by qPCR using the primers (forward, 5′-GCCTGAAGACAGTGGGGAAGG-3′; and reverse, 5′-CCACACTGGCTGGGAGTCTA-3′; the fragment is between −20 and +145).

Cell transfection and retroviral particle production and transduction

NIH 3T3 and BALB3T3 cells were transfected with 20 μg of pMYs-MZF1-IRES-EGFP or pMYs-IRES-EGFP plasmid by Lipofectamine 3000 (Invitrogen) in 10-cm dishes when the cells were 50–60% confluent. DNA samples (for ChIP analysis), protein lysates, and total RNAs were made 48 h post-transfection. Retroviruses expressing MZF1-GFP or GFP were prepared by adapting previously described methods (35). PlatE cells were transfected with pMYs-MZF1-IRES-EGFP or pMYs-IRES-EGFP plasmids by Lipofectamine 3000 (Invitrogen), and recombinant retroviral particles were collected 24–36 h after transfection. T1165 cells were transduced with retroviral particles by spin inoculation (2500 rpm for 90 min), cultured for 48 h, and then sorted for GFP-positive cells with BD FACSAria Violet (Flow Cytometry Core Facility, NCI, National Institutes of Health).

siRNA knockdown

siRNA-mediated knockdown of *Mzf1* was performed using the DharmaFECT 1 transfection reagent (horizon/Dharmacon, catalogue no. T-2001-02) according to the provided protocol. NIH 3T3 and BALB3T3 cells were transfected with mouse *Mzf1* siRNA (Thermo Fisher, siRNA code s99636, catalogue no. 4390771) at 25 nM final concentration in 6-well plates. The transfection medium was replaced with complete medium after 6–8 h, and incubation continued for an additional 48 h. At this point cells were collected and analyzed for mRNA and protein expression.

Bioinformatics and statistical analysis

Putative MZF1 CREs in the promoter of *Mtor* were predicted using MatInspector (Genomatix), and NRLB was used for generating the recognition model of the $\Delta\Delta G/RT$ coefficients for MZF1 *cis*-regulatory elements. All experiments were performed at least three times. Statistical significance of the differences between the control and treatment was analyzed by Student's *t* test. The data are presented as means ± S.D. *Error bars* represent the means ± S.E. The values were considered to be statistically significant when $p < 0.05$ (*) and $p < 0.01$ (**).

Author contributions—S. Z. and B. A. M. conceptualization; S. Z., W. S., E. S. R., V. B., A. M. E., D. C., M. S., W. D., and B. A. M. data curation; S. Z., W. S., E. S. R., V. B., A. M. E., W. D., and B. A. M. formal analysis; S. Z. and B. A. M. supervision; S. Z., W. S., V. B., A. M. E., D. C., and M. S. validation; S. Z., E. S. R., and B. A. M. investigation; S. Z., E. S. R., V. B., A. M. E., D. C., and B. A. M. visualization; S. Z., W. S., V. B., A. M. E., and B. A. M. methodology; S. Z., W. S., and B. A. M. writing-original draft; S. Z. and B. A. M. project administration; S. Z., W. S., and B. A. M. writing-review and editing; B. A. M. resources; B. A. M. funding acquisition.

Acknowledgments—We thank Dr. Douglas Lowy and anonymous reviewers for advice and careful reading of the manuscript. We thank Drs. Subhadra Banerjee and Shafluddin Siddiqui for cell sorting in the Flow Cytometry Core, Lab of Genome Integrity, NCI, National Institutes of Health. Our thanks also go to summer interns Jeffrey Chu and Olivia Cong for help in cell culture and transfection experiments. We also thank Dr. Ke Zhang for advice regarding our transfection experiments. We appreciate the support of the Center for Cancer Research Sequencing Facility for sequencing of plasmid constructs and Amy Zhang for assisting with GenBank™ submission of sequences.

References

1. Boutouja, F., Stiehm, C. M., and Platta, H. W. (2019) mTOR: a cellular regulator interface in health and disease. *Cells* **8,** E18 CrossRef Medline
2. Kim, J., and Guan, K. L. (2019) mTOR as a central hub of nutrient signalling and cell growth. *Nat. Cell Biol.* **21,** 63–71 CrossRef Medline
3. Saxton, R. A., and Sabatini, D. M. (2017) mTOR signaling in growth, Metabolism, and disease. *Cell* **168,** 960–976 CrossRef Medline
4. Nguyen, J. T., Ray, C., Fox, A. L., Mendonça, D. B., Kim, J. K., and Krebsbach, P. H. (2018) Mammalian EAK-7 activates alternative mTOR signaling to regulate cell proliferation and migration. *Sci. Adv.* **4,** eaao5838 CrossRef Medline
5. Bliskovsky, V., Ramsay, E. S., Scott, J., DuBois, W., Shi, W., Zhang, S., Qian, X., Lowy, D. R., and Mock, B. A. (2003) Frap, FKBP12 rapamycin-associated protein, is a candidate gene for the plasmacytoma resistance locus Pctr2 and can act as a tumor suppressor gene. *Proc. Natl. Acad. Sci. U.S.A.* **100,** 14982–14987 CrossRef Medline
6. Mock, B. A., Krall, M. M., and Dosik, J. K. (1993) Genetic mapping of tumor susceptibility genes involved in mouse plasmacytomagenesis. *Proc. Natl. Acad. Sci. U.S.A.* **90,** 9499–9503 CrossRef Medline
7. Zhang, S., Readinger, J. A., DuBois, W., Janka-Junttila, M., Robinson, R., Pruitt, M., Bliskovsky, V., Wu, J. Z., Sakakibara, K., Patel, J., Parent, C. A., Tessarollo, L., Schwartzberg, P. L., and Mock, B. A. (2011) Constitutive reductions in mTOR alter cell size, immune cell development, and antibody production. *Blood* **117,** 1228–1238 CrossRef Medline
8. Sintes, J., Gentile, M., Zhang, S., Garcia-Carmona, Y., Magri, G., Cassis, L., Segura-Garzón, D., Ciociola, A., Grasset, E. K., Bascones, S., Comerma, L., Pybus, M., Lligé, D., Puga, I., Gutzeit, C., *et al.* (2017) mTOR intersects antibody-inducing signals from TACI in marginal zone B cells. *Nat. Commun.* **8,** 1462 CrossRef Medline

9. Zhang, S., Pruitt, M., Tran, D., Du Bois, W., Zhang, K., Patel, R., Hoover, S., Simpson, R. M., Simmons, J., Gary, J., Snapper, C. M., Casellas, R., and Mock, B. A. (2013) B cell-specific deficiencies in mTOR limit humoral immune responses. *J. Immunol.* **191,** 1692–1703 CrossRef Medline
10. Nordan, R. P., and Potter, M. (1986) A macrophage-derived factor required by plasmacytomas for survival and proliferation *in vitro*. *Science* **233,** 566–569 CrossRef Medline
11. Morris, J. F., Hromas, R., Rauscher, F. J., 3rd (1994) Characterization of the DNA-binding properties of the myeloid zinc finger protein MZF1: two independent DNA-binding domains recognize two DNA consensus sequences with a common G-rich core. *Mol. Cell Biol.* **14,** 1786–1795 CrossRef Medline
12. Piszczatowski, R. T., Rafferty, B. J., Rozado, A., Tobak, S., and Lents, N. H. (2014) The glyceraldehyde 3-phosphate dehydrogenase gene (GAPDH) is regulated by myeloid zinc finger 1 (MZF-1) and is induced by calcitriol. *Biochem. Biophys. Res. Commun.* **451,** 137–141 CrossRef Medline
13. Rastogi, C., Rube, H. T., Kribelbauer, J. F., Crocker, J., Loker, R. E., Martini, G. D., Laptenko, O., Freed-Pastor, W. A., Prives, C., Stern, D. L., Mann, R. S., and Bussemaker, H. J. (2018) Accurate and sensitive quantification of protein–DNA binding affinity. *Proc. Natl. Acad. Sci. U.S.A.* **115,** E3692–E3701 CrossRef Medline
14. Weirauch, M. T., Yang, A., Albu, M., Cote, A. G., Montenegro-Montero, A., Drewe, P., Najafabadi, H. S., Lambert, S. A., Mann, I., Cook, K., Zheng, H., Goity, A., van Bakel, H., Lozano, J. C., Galli, M., *et al.* (2014) Determination and inference of eukaryotic transcription factor sequence specificity. *Cell* **158,** 1431–1443 CrossRef Medline
15. Hromas, R., Davis, B., Rauscher, F. J., 3rd, Klemsz, M., Tenen, D., Hoffman, S., Xu, D., and Morris, J. F. (1996) Hematopoietic transcriptional regulation by the myeloid zinc finger gene, MZF-1. *Curr. Top. Microbiol. Immunol.* **211,** 159–164 Medline
16. Moeenrezakhanlou, A., Shephard, L., Lam, L., and Reiner, N. E. (2008) Myeloid cell differentiation in response to calcitriol for expression CD11b and CD14 is regulated by myeloid zinc finger-1 protein downstream of phosphatidylinositol 3-kinase. *J. Leukoc. Biol.* **84,** 519–528 CrossRef Medline
17. Mudduluru, G., Vajkoczy, P., and Allgayer, H. (2010) Myeloid zinc finger 1 induces migration, invasion, and *in vivo* metastasis through Axl gene expression in solid cancer. *Mol. Cancer Res.* **8,** 159–169 CrossRef Medline
18. Morris, J. F., Rauscher, F. J., 3rd, Davis, B., Klemsz, M., Xu, D., Tenen, D., and Hromas, R. (1995) The myeloid zinc finger gene, MZF-l, regulates the CD34 promoter *in vitro*. *Blood* **86,** 3640–3647 Medline
19. Perrotti, D., Melotti, P., Skorski, T., Casella, I., Peschle, C., and Calabretta, B. (1995) Overexpression of the zinc finger protein MZF1 inhibits hematopoietic development from embryonic stem cells: correlation with negative regulation of CD34 and c-myb promoter activity. *Mol. Cell Biol.* **15,** 6075–6087 CrossRef Medline
20. Deng, Y., Wang, J., Wang, G., Jin, Y., Luo, X., Xia, X., Gong, J., and Hu, J. (2013) p55PIK transcriptionally activated by MZF1 promotes colorectal cancer cell proliferation. *BioMed. Res. Int.* **2013,** 868131 Medline
21. Vishwamitra, D., Curry, C. V., Alkan, S., Song, Y. H., Gallick, G. E., Kaseb, A. O., Shi, P., and Amin, H. M. (2015) The transcription factors Ik-1 and MZF1 downregulate IGF-IR expression in NPM-ALK(+) T-cell lymphoma. *Mol. Cancer* **14,** 53–70 CrossRef Medline
22. Eguchi, T., Prince, T., Wegiel, B., and Calderwood, S. K. (2015) Role and regulation of myeloid zinc finger protein 1 in cancer. *J. Cell Biochem.* **116,** 2146–2154 CrossRef Medline
23. Janku, F., Yap, T. A., and Meric-Bernstam, F. (2018) Targeting the PI3K pathway in cancer: are we making headway? *Nat. Rev. Clin. Oncol.* **15,** 273–291 CrossRef Medline
24. Grabiner, B. C., Nardi, V., Birsoy, K., Possemato, R., Shen, K., Sinha, S., Jordan, A., Beck, A. H., and Sabatini, D. M. (2014) A diverse array of cancer-associated MTOR mutations are hyperactivating and can predict rapamycin sensitivity. *Cancer Discov.* **4,** 554–563 CrossRef Medline
25. Cao, Q., Ju, X., Li, P., Meng, X., Shao, P., Cai, H., Wang, M., Zhang, Z., Qin, C., and Yin, C. (2012) A functional variant in the MTOR promoter modulates its expression and is associated with renal cell cancer risk. *PLoS One* **7,** e50302 CrossRef Medline
26. Xu, M., Tao, G., Kang, M., Gao, Y., Zhu, H., Gong, W., Wang, M., Wu, D., Zhang, Z., and Zhao, Q. (2013) A polymorphism (rs2295080) in mTOR promoter region and its association with gastric cancer in a Chinese population. *PLoS One* **8,** e60080 CrossRef Medline
27. Zining, J., Lu, X., Caiyun, H., and Yuan, Y. (2016) Genetic polymorphisms of mTOR and cancer risk: a systematic review and updated meta-analysis. *Oncotarget* **7,** 57464–57480 Medline
28. Bendavit, G., Aboulkassim, T., Hilmi, K., Shah, S., and Batist, G. (2016) Nrf2 transcription factor can directly regulate mTOR: linking cytoprotective gene expression to a major metabolic regulator that generates redox activity. *J. Biol. Chem.* **291,** 25476–25488 CrossRef Medline
29. Zhang, S. L., DuBois, W., Ramsay, E. S., Bliskovski, V., Morse, H. C., 3rd, Taddesse-Heath, L., Vass, W. C., DePinho, R. A., and Mock, B. A. (2001) Efficiency alleles of the Pctr1 modifier locus for plasmacytoma susceptibility. *Mol. Cell Biol.* **21,** 310–318 CrossRef Medline
30. Zhang, S., Qian, X., Redman, C., Bliskovski, V., Ramsay, E. S., Lowy, D. R., and Mock, B. A. (2003) p16 INK4a gene promoter variation and differential binding of a repressor, the ras-responsive zinc-finger transcription factor, RREB. *Oncogene* **22,** 2285–2295 CrossRef Medline
31. Villar, V. H., Nguyen, T. L., Terés, S., Bodineau, C., and Durán, R. V. (2017) Escaping mTOR inhibition for cancer therapy: tumor suppressor functions of mTOR. *Mol. Cell Oncol.* **4,** e1297284 CrossRef Medline
32. Villar, V. H., Nguyen, T. L., Delcroix, V., Terés, S., Bouchecareilh, M., Salin, B., Bodineau, C., Vacher, P., Priault, M., Soubeyran, P., and Durán, R. V. (2017) mTORC1 inhibition in cancer cells protects from glutaminolysis-mediated apoptosis during nutrient limitation. *Nat. Commun.* **8,** 14124 CrossRef Medline
33. Potter, M., and Boyce, C. R. (1962) Induction of plasma-cell neoplasms in strain BALB/c mice with mineral oil and mineral oil adjuvants. *Nature* **193,** 1086–1087 CrossRef Medline
34. Mock, B. A., Hartley, J., Le Tissier, P., Wax, J. S., and Potter, M. (1997) The plasmacytoma resistance gene, Pctr2, delays the onset of tumorigenesis and resides in the telomeric region of chromosome 4. *Blood* **90,** 4092–4098 Medline
35. Kitamura, T., Koshino, Y., Shibata, F., Oki, T., Nakajima, H., Nosaka, T., and Kumagai, H. (2003) Retrovirus-mediated gene transfer and expression cloning: powerful tools in functional genomics. *Exp. Hematol.* **31,** 1007–1014 CrossRef Medline